Dyes and Pigments 85 (2010) 66–72

Contents lists available at ScienceDirect

Dyes and Pigments

journal homepage: www.elsevier.com/locate/dyepig

High luminescence, organic–inorganic nanocomposite films with covalently linked 8-hydroxyquinoline anchored to ZnS nanoparticles

Yongli Shi [a], Yuqin Fu [b], Changli Lü [a,*], Li Hui [a], Zhongmin Su [a]

[a] Institute of Chemistry, Northeast Normal University, Changchun 130024, PR China
[b] College of Life Sciences, Jilin Agricultural University, Changchun 130118, PR China

ARTICLE INFO

Article history:
Received 25 June 2009
Received in revised form
3 October 2009
Accepted 5 October 2009

Keywords:
8-Hydroxyquinoline
ZnS nanoparticles
Organic–inorganic
Nanocomposites
Fluorescence
Polymer

ABSTRACT

A series of transparent, highly fluorescent, organic–inorganic nanocomposite films were prepared by incorporating mercaptoethanol-capped ZnS nanoparticles into a copolymer of trialkoxysilane-capped poly(MMA-co-Hq-CH_2-HEMA) carrying an 8-hydroxyquinoline (Hq) unit, followed by ligand exchange and sol–gel processing. Electron microscopy revelaed that the ZnS nanoparticles were uniformly dispersed in the organic–inorganic hybrid matrix regardless of the content and matrix composition. The hybrid nanocomposites had good optical transparency in the visible region. The nanocomposites that contained the ZnS nanoparticles were stable and displayed high fluorescence emission at 500 nm, which differed from that of hybrid materials obtained by simply blending the zinc ions or bis(8-hydroxyquinoline) zinc compound with the copolymer matrix. Thermogravimetric analysis indicated that the nanocomposite materials had high thermal stability.

1. Introduction

Since the first, efficient, low-voltage-driven, organic light-emitting diodes (OLEDs) based on tris(8-hydroxyquinoline) aluminium (Alq_3) were reported by Tang and co-workers in 1987 [1], 8-hydroxyquinoline (Hq) and its metalloquinolates have attracted great interest because their high thermal stability and good electroluminescence properties make them important prototypical electron transport and emitting materials for OLED devices [2–4]. Among the metalloquinolates, Alq_3 and zinc(II)-bis (8-hydroxyquinoline) (Znq_2) are typical representatives. The emission properties of the metalloquinolates can be tuned by the electronic nature of the arylethynyl substituents on the Hq ligand or by introducing optically inactive spacer molecules into their crystalline networks [5–9]. Generally, fabrication of device films for metal-quinoline chelates is carried out using vacuum-deposition [8,10] and, therefore, it is desirable to develop low-cost solution-processing techniques, such as spin-coating or ink-jet printing, for the large-scale fabrication of such devices [11–13].

The design and fabrication of novel organic–inorganic hybrids have been the focus of research for a long time [14–18]. Nowadays, most hybrid materials are synthesized using conventional chemistry and combine the properties of organic and inorganic components [18]. However, with the rapid development of nanoscience and nanotechnology, functional organic–inorganic hybrids of innovative multiscale and hierarchically organized structures offer potential application as photovoltaic and fuel cells, smart and bionic materials, catalysts and sensors as well as the next generation of optical and photoelectronic systems [18,19]. In this context, fluorescent components such as rare earth complexes [20–22], dyes [16,23], Alq_3 [24] and semiconductor quantum dots (QDs) [25] have been incorporated into hybrid systems using a sol–gel route to secure materials with high stability, excellent thermal stability and ease of processing.

This study concerns a facile route for the preparation of highly fluorescent hybrid nanocomposites from trialkoxysilane-capped poly(MMA-co-Hq-CH_2-HEMA) and mercaptoethanol (ME)-capped ZnS nanoparticles (NPs) via ligand exchange and sol–gel process. The novelty of this strategy is that the Hq molecules are used to attach to the surface of semiconductor NPs for the first time to fabricate the fluorescence organic–inorganic nanocomposites with Hq-containing copolymers through ligand exchange. The interaction between NPs and the metalloquinolates formed on the NPs surface may mainly contribute to the interesting highly photoluminescence properties. By using the design of the copolymer of trialkoxysilane-capped poly(MMA-co-Hq-CH_2-HEMA) in this paper, the integration of the luminescent function within the stable and processible organic–inorganic hybrids can be achieved by the sol–gel process.

* Corresponding author. Fax: +86 431 85098768.
E-mail addresses: lucl055@nenu.edu.cn (C. Lü), zmsu@nenu.edu.cn (Z. Su).

0143-7208/$ – see front matter © 2009 Elsevier Ltd. All rights reserved.
doi:10.1016/j.dyepig.2009.10.005

2. Experimental

2.1. Materials

Methyl methacrylate (MMA) and 3-(trimethoxysilyl) propyl methacrylate (MSMA) were distilled under reduced pressure before use. Azodiisobutyronitrile (AIBN) was recrystallized in ethanol. 5-(2-Methacryloylethyloxymethyl)-8-quinolinol (Hq-CH_2-HEMA) was synthesized as reported previously [13]. Tetrahydrofuran (THF) was dried by refluxing over metal sodium before use. 2-Mercaptoethanol (ME), zinc acetate dihydrate, thiourea and N, N-dimethylformamide (DMF) were all analytical grade reagents and were used without further purification. Bis(8-hydroxyquinoline) zinc (Znq_2) was synthesized according to the reported method [26].

2.2. Characterization

FTIR spectra were recorded on a Magna 560 FTIR spectrometer. The molecular weights of the polymers were determined by gel permeation chromatography (GPC) equipped with Waters 1515 pump and Waters 2414 differential refractive index detector. The eluent was THF at a flow rate of 1.0 mL/min. A series of low polydispersity polystyrene standards were employed for the GPC calibration. Transmission electron microscopy (TEM) was carried out on a JEOL-2021 microscope. UV–vis spectra were recorded on a Vary 500 UV-vis-NIR spectrometer in the range of 200–800 nm. Photoluminescence spectra were measured on a Cary Eclipse fluorescence spectrometer. Thermogravimetric analysis (TGA) was performed on a Perkin–Elmer TGA-2 thermogravimetric analyzer under a nitrogen atmosphere at a heating rate of 20 °C min^{-1}.

2.3. Synthesis of trialkoxysilane-capped poly(MMA-co-Hq-CH_2-HEMA) copolymer

A mixture of MMA (4.0 g), MSMA (0.95 g), HEMA-CH_2-Hq (0.05 g), AIBN (0.03 g) and anhydrous THF (25 mL) was placed in a 100 mL three-neck round bottom flask fitted with a magnetic stirrer and a reflux condenser under nitrogen atmosphere. The reaction solution was kept at 60 °C for 20 h with stirring. A THF solution of the copolymer with a solid content of 28 wt% was obtained. The copolymer was precipitated several times by using ether and a white powder was obtained. The number-average molecular weight (M_n) of this copolymer was determined to be 31 800 [polydispersity index, M_w/M_n = 1.52] by the GPC. The copolymer of p(MMA-MSMA) with a weight ratio of 80:20 for MMA to MSMA was synthesized through a similar process as mentioned above. The M_n and M_w/M_n of this copolymer are 48 500 and 2.53, respectively. Fig. 1 is the synthetic routes for these copolymers.

2.4. Preparation of mercaptoethanol (ME) capped ZnS (ME-ZnS) NPs

ME-ZnS nanoparticles (NPs) were prepared in DMF solution using the similar method reported earlier [27]. In a typical experiment, zinc acetate dihydrate (16.5 g, 75.3 mmol), thiourea (5.2 g, 68.3 mmol) and ME (8.7 g, 111.4 mmol) were dissolved in 150 mL DMF. The solution was stirred at 155–160 °C for 10 h under nitrogen atmosphere. The reaction solution was concentrated to about 50 mL at a reduced pressure, and then the resulting solution was poured into 200 mL ethanol and the formed white precipitate was collected by centrifugation. The white powder was thoroughly washed several times with methanol and then dried in vacuum.

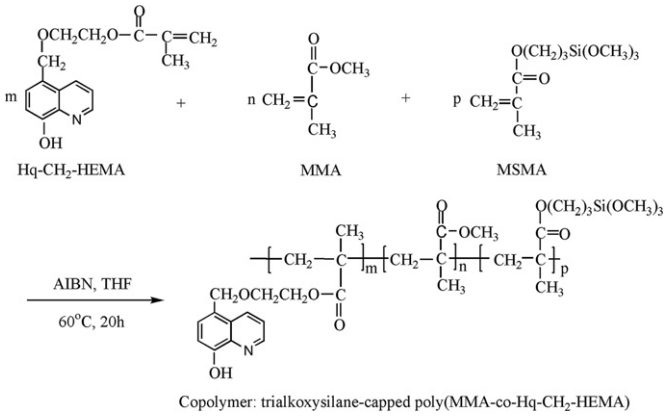

Fig. 1. Synthetic scheme for the copolymer of trialkoxysilane-capped poly (MMA -co-Hq-CH_2-HEMA).

2.5. Preparation of polymer nanocomposite films

For p-ZnSX-SiY samples, ZnS NPs dispersed in DMF were added into the copolymer solution of trialkoxysilane-capped poly(MMA-co-Hq-CH_2-HEMA). After the mixture solution was kept under ultrasonic vibration for 5 min, TEOS and water was added (the molar ratio of -Si-OR in copolymer and TEOS to H_2O is 0.625:1). The reaction solution was stirred for 8 h at room temperature, and then the solution was spin-coated on a quartz wafer at 3000 rpm for 30 s. The quartz wafer was pretreated with sulfuric acid and hydrogen peroxide. The solid content of the coating solution is about 5 wt%. The films were cured at 60 °C for 3 h, 80 °C for 1 h, 100 °C for 1 h, 120 °C for 1 h and 100 °C under vacuum for 1 h. For p-ZnS samples, except without use of TEOS, all the other conditions are similar to that of the synthesis for p-ZnSX-SiY samples. The zinc ion (acetate dihydrate as zinc salt) was also introduced into the sol–gel systems to prepare the hybrid samples of p-Zn^{2+}(2:1), p-Zn^{2+}(1:1) and p-Zn^{2+}-Si20 (see Table 1). Here, the molar ratio of Hq-CH_2-HEMA units in the copolymer to Zn ions is 2:1 and 1:1 respectively, and the SiO_2 weight content in the resulting hybrids is fixed at 20 wt%. The p-Znq_2 hybrid sample was also prepared by blending Znq_2 complex with the copolymer of poly(MMA-MSMA) in THF solution, followed by the same procedure mentioned above. The weight content of Znq_2 complex in hybrid is similar to that of p-Zn^{2+}(2:1) (0.61 wt%). The thickness of the above hybrid films was controlled at about 1.0 μm.

Table 1
Some properties of the organic–inorganic hybrid nanocomposite films.

Sample[a]	λ_{ex}[b] (nm)	λ_{em}[c] (nm)	T (%)[d]	T_d (°C)[e]	Residue (wt%)[f]
P(copolymer)	–	–	99.2	294	15.1(4.6)
p-ZnS1	370	495	96.4	292	27.5(23.0)
p-ZnS3	373	500	98.2	281	20.4(12.3)
p-ZnS10	369	500	98.4	249	19.2(7.2)
p-Zn^{2+}(1:1)	370	501	–	–	–
p-Zn^{2+}(2:1)	370	492	–	227	17.8(4.7)
p-Znq_2	378	515	–	227	16.0(4.8)
p-ZnS3-Si10	372	499	98.1	307	24.5(21.0)
p-ZnS3-Si40	372	500	98.8	301	57.0(47.2)

[a] P-ZnSX-SiY is defined as a nanocomposite with X weight percent of Hq unit in copolymers to ZnS NPs and Y weight percent of silica in nanocomposites.
[b] Maximum excitation wavelength.
[c] Maximum emission peak positions.
[d] Transmittance at 450 nm.
[e] 5 wt% decomposition temperatures.
[f] Char yield at 785 °C after TGA (Theoretical char yield).

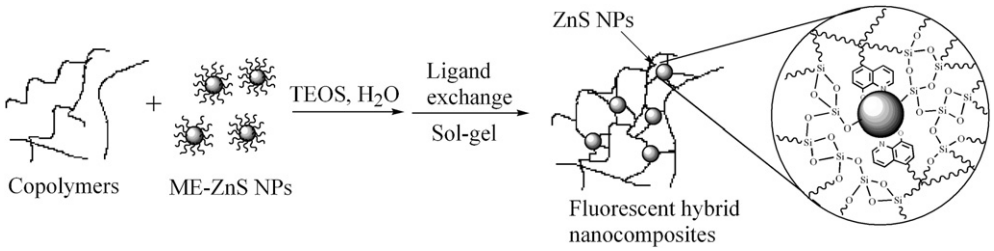

Fig. 2. Preparative scheme of highly fluorescent hybrids by ligand exchange and sol–gel process.

3. Results and discussion

The copolymer of trialkoxysilane-capped poly(MMA-co-Hq-CH_2-HEMA) was synthesized from the monomers of MMA, MSMA and Hq-CH_2-HEMA with a weight ratio of 80:19:1. The synthesis procedure of this copolymer is illustrated in Fig. 1. GPC analysis revealed that the number-average molecular weight (M_n) of the copolymer were 31 800 ($M_w/M_n = 1.52$). The highly fluorescence organic–inorganic nanocomposite films were fabricated from the ME-capped ZnS NPs and Hq-containing copolymer hybrid sols through the combined use of ligand exchange and sol–gel route (see Fig. 2). Herein we have prepared two series of hybrid films of

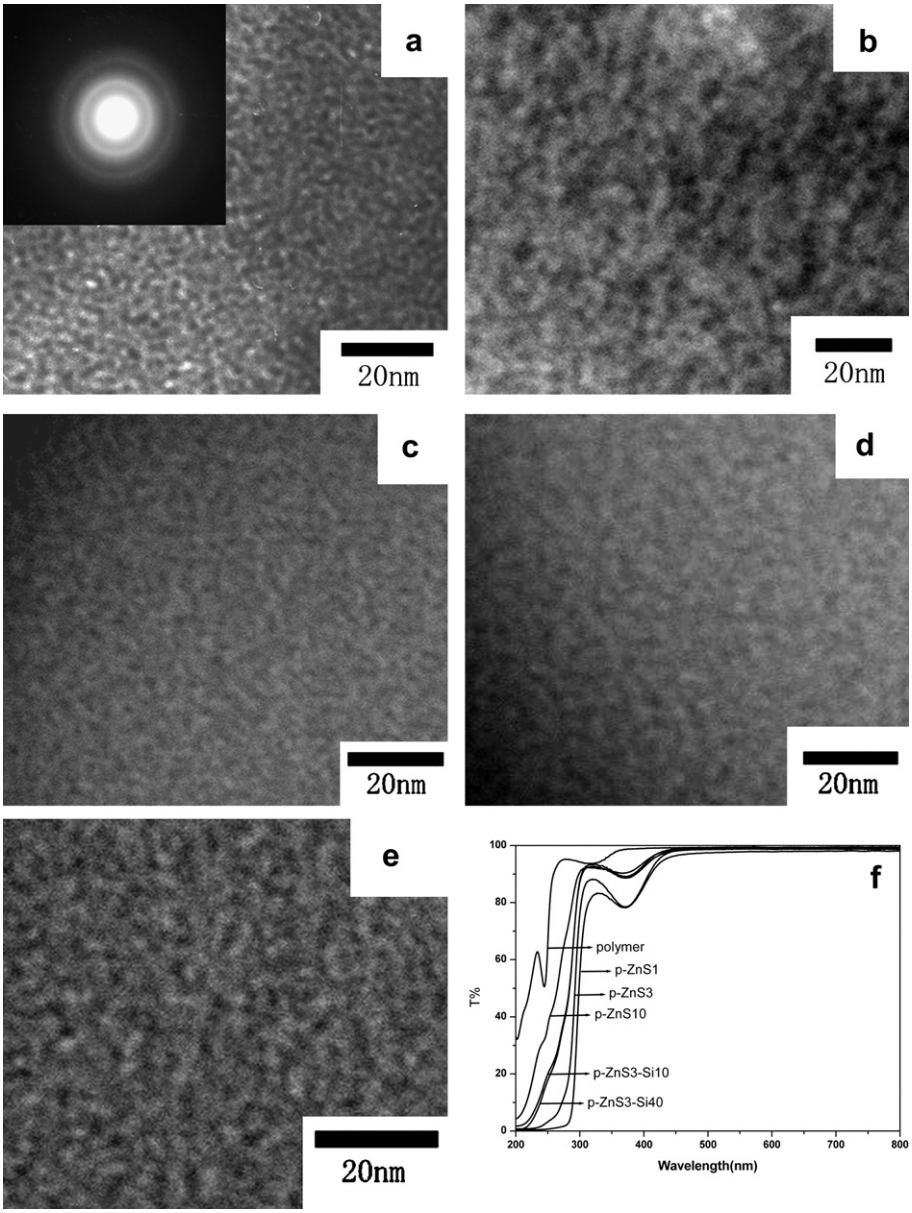

Fig. 3. TEM images of (a) ZnS NPs and nanocomposites of (b) p-ZnS3, (c) p-ZnS10, (d) p-ZnS3-Si10, (e) p-ZnS3-Si40, and (f) UV–vis transmittance spectra of nanocomposites. Inset in Fig. 3a is the selected area electron diffraction pattern of ZnS NPs.

p-ZnSX and p-ZnSX-SiY (see Table 1). In addition, to compare the optical properties, the Znq_2-polymer and Zn^{2+}-polymer hybrids were also synthesized by directly blending Znq_2 complex and zinc acetate dihydrate with the copolymer sols, followed by a programmed heating process.

Fig. 3a–e shows the TEM images of ZnS NPs, p-ZnS3, p-ZnS10, p-ZnS3-Si10 and p-ZnS3-Si40 samples. The selected area electron diffraction (see inset in Fig. 1a) of ZnS NPs displays the broad diffuse rings with (111), (220), (311), (420) and (422) planes for the cubic structure of sphalerite ZnS. The ZnS NPs are uniformly dispersed before and after immobilization in the hybrid matrix and maintain their original size (about 3 nm) without aggregation regardless of the content of NPs and matrix composition. The UV–vis transmittance spectra (Fig. 3f) indicate that the nanocomposites have good transparency in the visible region of the electromagnetic spectrum. The T% of the hybrid nanocomposites can reach as high as 96% at above 450 nm (Table 1). Although the p-ZnS1 exhibits a lowest transmittance on the whole, its T% is still above 85% at the visible region (400–800 nm). The apparent decrease in optical transmittance of the nanocomposites below 450 nm mainly results from the characteristic absorption of the ZnS nanoparticles in this region. The above results indicate that there is good compatibility between ZnS NPs and polymer hybrid matrix without obvious microphase separation because the organic moieties are covalently linked to the ZnS NPs by forming C–O–Si bonding between the hydroxyl groups of mercaptoethanol on ZnS surface and –Si-OH in silica precursors in the sol–gel process, besides the coordination effect of the Hq moiety in polymer chains (see Fig. 2). The FTIR study has confirmed the above result. Fig. 4 shows the FTIR spectra of ZnS NPs and different NPs–polymer nanocomposites. It can be seen that there are obvious O–H bands at about 3400 cm^{-1} due to the existence of the hydroxyl groups on ZnS surface and uncondensed hydroxyl groups of triethoxysilicane moieties in the copolymer chains. However, when the ZnS NPs are incorporated into the copolymers, the absorption intensity of the hydroxyl groups in this region obviously decreases for the nanocomposites, especially for the p-ZnS10 sample, indicating that the partially or full co-condensation reaction has occurred between the hydroxyl groups on the ZnS surface and silica precursors in the polymerization systems.

Fig. 5a shows the photoluminescence (PL) spectra of different hybrid samples, ZnS NPs and Znq_2 complex in solid state films. The maximum excitation and emission peak positions of the hybrid

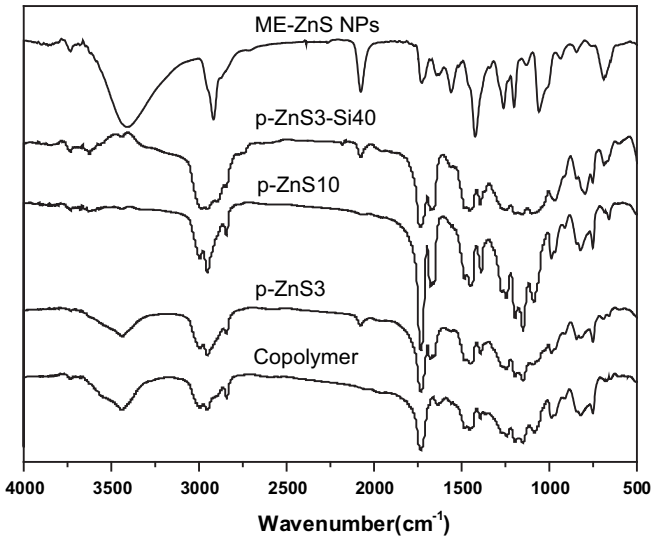

Fig. 4. FTIR spectra of ZnS NPs and different polymer hybrid samples.

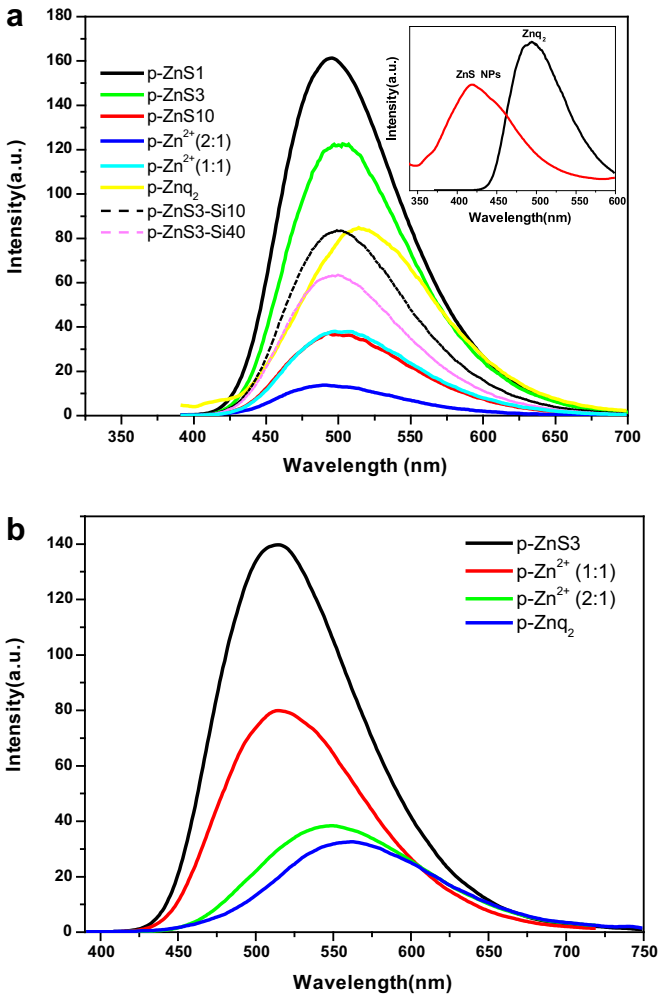

Fig. 5. PL spectra of different hybrid samples in solid state film (a) and in DMF solution (b) at the excitation wavelength of 370 nm. Inset in Fig. 5a is the PL spectra of ZnS NPs and Znq_2 powders at the excitation wavelength of 310 nm and 370 nm, respectively.

samples are listed in Table 1. The weak blue emission at 420 nm for ZnS NPs is attributed to the defect-state recombination on the surface of ZnS NPs [27]. When ZnS NPs are incorporated into the copolymers, the obtained nanocomposites of p-ZnS1, p-ZnS3 and p-ZnS10 show a green fluorescent emission centered at about 500 nm. The emission peaks of the nanocomposites also red-shift slightly with increasing weight ratio of the copolymers with Hq units to ZnS NPs from 495 nm for p-ZnS1 to 500 nm for p-ZnS3, and the emission peak position does not further change when the weight percent is above 3%. In addition, the decrease in PL intensities of the nanocomposites with increasing weight ratio of Hq unit to ZnS NPs is possibly because of the concentration-quenching effect of the formed metalloquinolates on the surface of NPs. In order to compare the PL property, the zinc ions and Znq_2 were also introduced into the corresponding copolymers to prepare p-Zn^{2+}(1:1), p-Zn^{2+}(2:1) and p-Znq_2 hybrid films. It can be seen that the sample of p-Zn^{2+}(1:1) has the almost identical emission peak at about 500 nm. The p-Zn^{2+} (2:1) exhibits a very weak fluorescent emission at 492 nm, and an obvious red-shifted emission at 515 nm is also observed for p-Znq_2 when compared with that (494 nm) of Znq_2 complex. We also studied the PL behaviors in DMF solution for the samples of p-Zn^{2+}(1:1), p-Zn^{2+}(2:1), p-Znq_2 and p-ZnS3 (see Fig. 5b). The PL emission peaks of these samples in solution red-shift as compared with that of their corresponding solid state film samples due to the solvent effect. The maximum PL

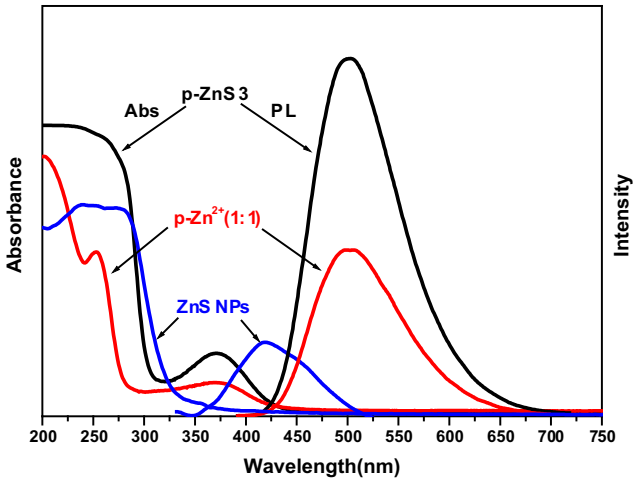

Fig. 6. Uv-vis absorption and PL spectra of different samples.

shift of about 50 nm is observed for p-Zn^{2+} (2:1) and p-Znq_2, while the PL peak shift of the samples p-ZnS3 and p-Zn^{2+} (1:1) is only about 10 nm. In particular, we should note that the samples of p-ZnS3 and p-Zn^{2+} (1:1) still have identical emission wavelength in DMF solution such as in their solid state films. This result indirectly confirms that the coordination structure of 8-hydroxyquinoline (Hq) unit in copolymer to zinc atom in p-ZnS3 is similar to that in p-Zn^{2+} (1:1), that is to say the molar ratio of Hq unit to the zinc atom on ZnS surface should be 1:1. The formation of single coordination bond for the metaloquinolate complexes on the surface of ZnS NPs in p-ZnS3 may be mainly responsible for the steric hindrance effect provided by the special spherical surface of NPs and the existence of Zn–S bonds as compared with the conventional coordination compounds such as Znq_2 complex. Recently, Bohle et al. studied the optical behavior of ZnO nanocrystals with surface-bound 8-hydroxyquinoline in solution [28]. The result also revealed that the Hq was attached to the surface of ZnO NCs in a 1:1 coordination fashion.

Although the PL peak positions of p-Zn^{2+} and p-Znq_2 are similar to that of p-ZnS the hybrid films of p-ZnS1 and p-ZnS3 present more strong PL emission in both solution and solid state films, indicating that the PL behavior of ZnS-copolymer hybrid systems should be different from that of pure ZnS NPs, p-Zn^{2+} and p-Znq_2. It is known that the optical properties of semiconductor NPs not only can be tuned by changing the particle size or by doping with suitable ions [29], but also by the surface functionalization using organic functional ligands or chromophores [30]. ZnS NPs have a great number of surface metal atoms that can coordinate with Hq unit in copolymer chains to form stable fluorescent complexes on the surface of NPs [27]. However, the above results indicate that the PL properties of ZnS-copolymer hybrid nanocomposites are not simply derived from the metaloquinolate complexes formed on the surface of ZnS NPs by the coordination effect of Hq unit to the surface zinc ions. Firstly, the unconventional metaloquinolate complexes on the spherical surface with a steric confinement effect can reduce the attack of water or oxygen, thus avoiding the leaching and quenching effects in the sol–gel systems [31,32], which results in the stronger PL emission of the nanohybrid materials than that of the conventional metaloquinolate complexes. In addition, the inherent luminescent emission of ZnS NPs may have a cooperative interaction with that of the metaloquinolate complexes on the surface of NPs. Actually, the PL mechanism of p-Zn^{2+} and p-Znq_2 is consistent with that of conventional small molecular Alq_3 or Znq_2 complexes. These samples display ligand-centered excited states and their fluorescent emission originates from the electronic $\pi-\pi^*$ charge transfer from the electron rich phenoxide ring to the electron deficient pyridyl ring in the quinolinolate ligands [33]. However, the emission properties of the metallocomplexes are in general controlled by the coordination fashion and angles that affect the energy mixing, and splitting of electronic states involved in the emission [6,7]. So, the PL properties between p-Zn^{2+} (1:1) and p-Zn^{2+} (2:1) are different due to the above affecting factor. For p-ZnS, there are two emission centers, including the inherent luminescent emission of ZnS NPs and the metaloquinolate complexes formed on the surface of NPs. The later emission mechanism is similar to that of the sample of p-Zn^{2+} (1:1). The PL behavior of p-ZnS also may be from the cooperative effect of the two PL emission centers because the obvious enhanced PL emission was observed in p-ZnS1 or p-ZnS3 as compared with other samples. In order to well understand this speculation, we compare the Uv-vis absorption and PL spectra of ZnS NPs, p-ZnS3 and p-Zn^{2+} (1:1) (see Fig. 6). The ZnS NPs exhibit a typical blue shift of nano-ZnS for absorption onset as compared with that of bulk ZnS (335 nm, 3.7 eV) [34]. For p-ZnS3, there is an absorption band centered at 375 nm similar to that of p-Zn^{2+} (1:1) besides the intrinsic absorption of ZnS NPs. This band should be assigned to the charge transfer transition from oxide containing phenolato moiety of the quinolate ligand to its nitrogen-containing pyridyl moiety [35]. This result indicates that the Hq units in copolymer are anchored to the surface of ZnS NPs to form the metalloquinolates. It is also should be noted that there is a spectral overlap between the emission band of ZnS NPs and the absorption band of p-Zn^{2+} (1:1). So, we consider that the fluorescent enhancement of the hybrid materials such as p-ZnS3 may partially attributed to the förster energy transfer from the ZnS NPs (donor) to the metaloquinolate complexes (acceptor) formed on the surface of NPs [36]. Further study is required to well understand the mechanism affecting the optical properties of the hybrid nanocomposites.

To improve the mechanical and thermal properties of the resulting nanocomposites, the samples of p-ZnS3-Si10 and p-ZnS3-Si40 were also prepared by introducing inorganic SiO_2 in the hybrid networks. From the PL spectra (Fig. 5a), it can be seen that the two nanocomposites still possess good fluorescence emission properties at 500 nm. The decline of the emission intensities of the nanocomposites may be due to the concentration decrease of the fluorescent components with increasing silica content when

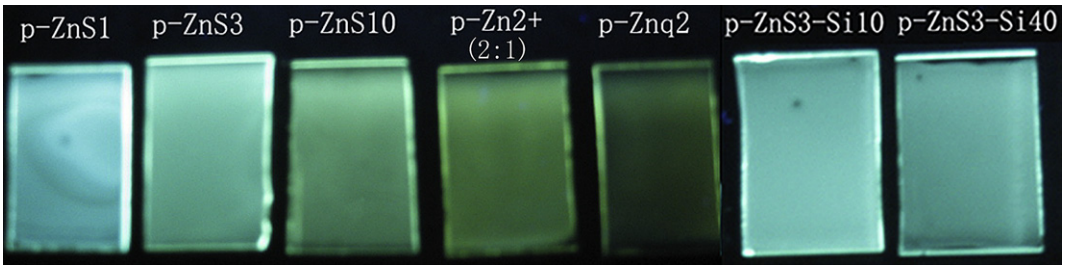

Fig. 7. PL images of different fluorescent hybrid films excited by an UV lamp with 360 nm.

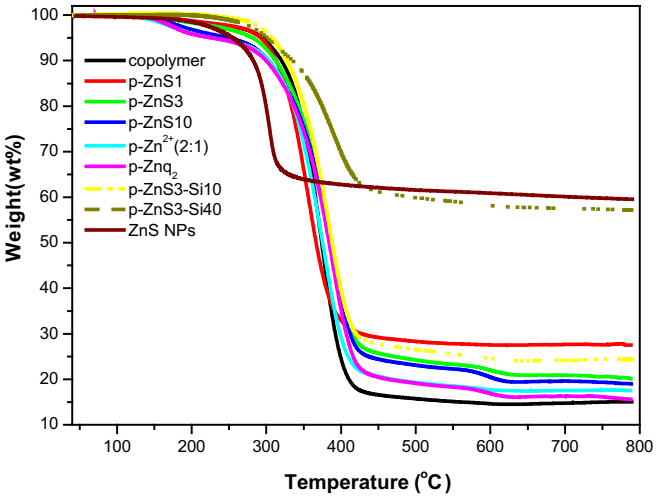

Fig. 8. TGA curves of different hybrid samples.

compared with p-ZnS3 sample. Fig. 7 shows the PL images of different fluorescent hybrid films excited by an UV lamp with 360 nm.

The thermal properties of the fluorescent nanocomposites were studied and their typical TGA curves are shown in Fig. 8. These materials exhibit well thermal stability (see Table 1). The thermal decomposition temperatures (T_d) at 5% weight loss for these nanocomposites are between 220 and 310 °C, and these values are relative to the decomposition of the partial organic polymer matrix and the surface capping agents of ZnS particle surface. However, it should be noted that the T_d of the nanocomposites is obviously higher than that of the samples of p-Zn^{2+}, p-Znq_2 and ZnS NPs. As shown in FTIR spectra (Fig. 4), the covalent bonding formed between the polymer and nanoparticles partially improves the thermal stability of the nanohybrid materials, especially with high particle loading. When the inorganic silica phase was introduced into the hybrid materials, the T_d of the nanocomposites can be further improved. For examples, the T_d of p-ZnS3-Si10 and p-ZnS3-Si40 nanocomposites has reached above 300 °C. So it can be seen that the obtained high fluorescent nanohybrid materials by our strategy have excellent thermal stability as compared with that based on the conventional blending method. The residues of the hybrid samples at 785 °C are higher than the theoretical contents of the inorganic phase. The reason may be that the covalent linkages between the organic and inorganic phases trapped the organic moieties in the inorganic phase [37].

4. Conclusions

In conclusion, we have designed and synthesized the novel nanocomposites with ZnS NPs covalently bonded to the polymer hybrid matrix with 8-hydroxyquinoline ligand unit and inorganic silica network by ligand exchange and sol–gel approach. This facile strategy can endow the resultant nanocomposites with highly fluorescence, outstanding thermal stability and flexible processability. These fluorescent nanohybrid materials can be potentially used to fabricate multifunctional devices with novel photoelectric properties.

Acknowledgements

We would like to appreciate the financial support of National Natural Science Foundation of China (Nos.20704004), Training Fund of NENU'S Scientific Innovation Project (NENU-STC07003 and NENU-STB07007) and Analysis and Testing Foundation of Northeast Normal University.

References

[1] Tang CW, VanSlyke SA. Organic electroluminescent diodes. Applied Physics Letters 1987;51:913–5.
[2] Shen ZL, Burrows PE, Bulović V, Forrest SR, Thompson ME. Three-color, tunable, organic light-emitting devices. Science 1997;276:2009–11.
[3] Aziz H, Popovic ZD, Hu NX, Hor AM, Xu G. Degradation mechanism of small molecule- based organic light-emitting devices. Science 1999;283:1900–2.
[4] Barth S, Müller P, Riel H, Seidler PF, Rieß W, Vestweber H, et al. Electron mobility in tris(8- hydroxylquinoline) aluminum thin films determined via transient electroluminescence from single- and multilayer organic light-emitting diodes. Journal of Applied Physics 2001;89:3711–9.
[5] Brinkmann M, Gadre G, Muccini M, Taliani C, Masciocchi N, Sironi A. Correlation between molecular packing and optical properties in different crystalline polymorphs and amorphous thin films of mer-tris(8-hydroxyquinoline) aluminum(III). Journal of the American Chemical Society 2000;122:5147–57.
[6] Pohl R, Anzenbacher Jr P. Emission color tuning in AlQ_3 complexes with extended conjugated chromophores. Organic Letters 2003;5:2769–72.
[7] Pohl R, Montes VA, Shinar J, Anzenbacher Jr P. Red-green-blue emission from tris(5-aryl-8- quinolinolate) Al (III) complexes. Journal of Organic Chemistry 2004;69:1723–5.
[8] Chen C, Shi J. Metal chelates as emitting materials for organic electroluminescence. Coordination Chemistry Reviews 1998;171:161–74.
[9] Palacios MA, Wang Z, Montes VA, Zyryanov GV, Hausch BJ, Jursíková K, et al. Hydroxyquinolines with extended fluorophores: arrays for turn-on and ratiometric sensing of cations. Chemical Communications 2007:3708–10.
[10] Friend RH, Gymer RW, Holmes AB, Burroughes JH, Marks RN, Taliani C, et al. Electroluminescence in conjugated polymers. Nature 1999;397:121–8.
[11] Meyers A, Weck M. Solution and solid-state characterization of Alq_3-functionalized polymers. Chemistry of Materials 2004;16:1183–8.
[12] Wang XY, Weck M. Poly(styrene)-supported Alq_3 and BPh_2q. Macromolecules 2005;38:7219–24.
[13] Du N, Tian R, Peng J, Lu M. Synthesis and photophysical characterization of the free-radical copolymerization of metaloquinolate-pendant monomers with methyl methacrylate. Journal of Polymer Science: Part A: Polymer Chemistry 2005;43:397–406.
[14] Novak BM. Hybrid nanocomposite materials-between inorganic glasses and organic polymers. Advanced Materials 1993;5:422–33.
[15] Kickelbick G. Concepts for the incorporation of inorganic building blocks into organic polymers on a nanoscale. Progress in Polymer Science 2003;28:83–114.
[16] Sanchez C, Lebeau B, Chaput F, Boilot J-P. Optical properties of functional hybrid organic–inorganic nanocomposites. Advanced Materials 2003;15:1969–94.
[17] Pénard A-L, Gacoin T, Boilot J-P. Functionalized sol–gel coatings for optical applications. Accounts of Chemical Research 2007;40:895–902.
[18] Sanchez C, Julián B, Belleville P, Popall M. Applications of hybrid organic–inorganic nanocomposites. Journal of Materials Chemistry 2005;15:3559–92.
[19] Gómez-Romero P, Sanchez C. Hybrid materials. Functional properties. From maya blue to 21st century materials. New Journal of Chemistry 2005;29:57–8.
[20] Dong D, Jiang S, Men Y. Nanostructured hybrid organic–inorganic lanthanide complex films produced in situ via a sol–gel approach. Advanced Materials 2000;12:646–9.
[21] Li HR, Lin J, Zhang HJ, Fu LS, Meng QG, Wang SB. Preparation and luminescence properties of hybrid materials containing europium(III) complexes covalently bonded to a silica matrix. Chemistry of Materials 2002;14:3651–5.
[22] Sui YL, Yan B. Fabrication and photoluminescence of molecular hybrid films based on the complexes of 8-hydroxyquinoline with different metal ions via sol–gel process. Journal of Photochemistry and Photobiology A: Chemistry 2006;182:1–6.
[23] Avnir D, Levy D, Reisfeld R. The nature of the silica cage as reflected by spectral changes and enhanced photostability of trapped rhodamine 6G. Journal of Physical Chemistry 1984;88:5956–9.
[24] Zeng H, Huang W, Shi J. A covalently bonded AlQ_3/SiO_2 hybrid material with blue light emission by a conventional sol–gel approach. Chemical Communications 2006:880–1.
[25] Wang Q, Iancu N, Seo D-K. Preparation of large transparent silica monoliths with embedded photoluminescent CdSe@ZnS core/shell quantum dots. Chemistry of Materials 2005;17:4762–4.
[26] Xu B, Hao Y, Wang H, Zhou H, Liu X, Chen M. The effects of crystal structure on optical absorption/photoluminescence of bis(8-hydroxyquinoline)zinc. Solid State Communications 2005;136:318–22.
[27] Gao J, Lü C, Lü X, Du Y. APhen-functionalized nanoparticles-polymer fluorescent nanocomposites via ligand exchange and in situ bulk polymerization. Journal of Materials Chemistry 2007;17:4591–7.
[28] Bohle D, Spina C. Chelating the surface of zinc in zinc oxide nanocrystals: spectroscopic characterization of ZnO surface-bound eriochrome black T and 8-hydroxyquinoline. Journal of Physical Chemistry C 2009;113:14435–9.

[29] Xu SJ, Chua SJ, Liu B, Gan LM, Chew CH, Xu GQ. Luminescence characteristics of impurities-activated ZnS nanocrystals prepared in microemulsion with hydrothermal treatment. Applied Physics Letters 1998;73:478–80.
[30] Jin T, Fujii F, Yamada E, Nodasaka Y, Kinjo M. Control of the optical properties of quantum dots by surface coating with calix[n]arene carboxylic acids. Journal of the American Chemical Society 2006;128:9288–9.
[31] Papadimitrakopoulos F, Zhang X, Thomsen D, Higginson K. A chemical failure mechanism for aluminum(III) 8-hydroxyquinoline light-emitting devices. Chemistry of Materials 1996;8:1363–5.
[32] Papadimitrakopoulos F, Zhang X. Environmental stability of aluminum tris(8-hydroxyquinoline) (Alq_3) and its implications in light emitting devices. Synthetic Metals 1997;85:1221–4.
[33] Li N, Li X, Wang W, Geng W, Qiu S. Blue-shifting photoluminescence of Tris (8-hydroxy- quinoline) aluminium encapsulated in the channel of functionalized mesoporous silica SBA-15. Materials Chemistry and Physics 2006;100:128–31.
[34] Lippens PE, Lannoo M. Calculation of the band gap for small CdS and ZnS crystallites. Physical Review B 1989;39:10935–42.
[35] Burrows PE, Shen Z, Bulovic V, McCarty DM, Forrest SR. Relationship between electroluminescence and current transport in organic heterojunction light-emitting devices. Journal of Applied Physics 1996;79:7991–8006.
[36] Warner J, Watt A, Thomsen E, Heckenberg N, Meredith P, Rubinsztein-Dunlop H. Energy transfer dynamics of nanocrystal-polymer composites. Journal of Physical Chemistry B 2005;109:9001–5.
[37] Lee LH, Chen WC. High-refractive-index thin films prepared from trialkoxysilane-capped poly(methyl methacrylate)–titania materials. Chemistry of Materials 2001;13:1137–42.